Catena 139 (2016) 1–8

Contents lists available at ScienceDirect

Catena

journal homepage: www.elsevier.com/locate/catena

Application of HYDRUS-1D model to provide antecedent soil water contents for analysis of runoff and soil erosion from a slope on the Loess Plateau

Yi Caiqiong, Fan Jun *

State Key Laboratory of Soil Erosion and Dryland Farming on the Loess Plateau, Northwest A&F University, Yangling, Shaanxi 712100, China

ARTICLE INFO

Article history:
Received 22 April 2015
Received in revised form 17 November 2015
Accepted 30 November 2015
Available online 15 December 2015

Keywords:
HYDRUS-1D
Rainfall
Runoff
Soil water content

ABSTRACT

Aims: Antecedent soil water content (ASWC) is an important factor affecting soil water infiltration, runoff and soil erosion on slopes but it is difficult to measure or forecast accurately and is not often reported in soil erosion databases.
Methods: Runoff plots (12 m × 5 m) were used to collect runoff and sediment during the rainy seasons between April 2010 and October 2013 on the Loess Plateau, China. The HYDRUS-1D model was calibrated and tested using the data collected from the plots. The relationships of ASWC with runoff and sediment yield were investigated using the model output values for ASWC.
Results: The model performance was satisfactory, with a mean Nash–Sutcliffe model efficiency coefficient of 0.411 and a root mean square error of 0.031 during the four study years. Runoff was directly affected by rainfall amount and rain intensity. Furthermore, runoff typically increased with ASWC.
Conclusions: HYDRUS-1D can provide temporal ASWC data that could be used for runoff prediction.

1. Introduction

Soil erosion is an important global environmental problem that markedly influences the environment and social development (Fu et al., 2011; Higgitt, 1991). The Loess Plateau has long suffered from the most severe soil loss and runoff in China (Fu et al., 2009; Ni et al., 2004; Zheng, 2006), which has led to land and environmental degradation within the region and beyond, since sediments and pollutants can travel beyond its boundaries (An et al., 2008). Many studies have investigated the impact of antecedent soil water content (ASWC) on soil erosion and nutrient loss (Brocca et al., 2008; Huet et al., 2012; Mamedov et al., 2006; Paola et al., 2013; Qiu et al., 2001). Duiker et al. (2000) found that ASWC was the most effective factor when determining sediment yield. Vahabi and Nikkami (2008) reported that the effects of both vegetation cover and ASWC determined sediment yield from the Taleghan watershed in Iran, where soil textures ranged from light to heavy on slopes of 12% to 30% under different vegetation covers (9% to 49%). The ASWC influences water infiltration, which in turn affects the occurrence of runoff and erosion (Gao et al., 2011). Wei et al. (2007a) found that, with increasing ASWC at a depth of 10 cm, there was a reduction in water infiltration and experimental plots produced more runoff and sediments. Runoff production is a function of changes in both the soil surface in response to wetting and the rate of application of water to the soil surface (Bowyer-Bower, 1993). The ASWC parameter has been added to the criteria for the Soil Conservation Service-Curve Number (SCS-CN) in order to improve runoff estimation (Huang et al., 2007; Lal et al., 2015). The influence of ASWC on soil erosion has increasingly been considered in order to obtain more accurate estimates of soil losses.

There is a variety of ways by which to measure soil water content. Commonly used instruments for measuring soil water content are neutron probes (Huo et al., 2008) and time domain reflectometers (TDR) (Brocca et al., 2009; Gao et al., 2011). However, the use of TDR may not be suitable for multiple site observations in the field due to the expensive equipment (Calamita et al., 2012). Long-term monitoring of soil water content can provide the antecedent water content before a number of rainfall events (Gao et al., 2011; Qiu et al., 2003). However, soil water content monitoring at the watershed scale is difficult because of its space-time variability and because field measurements are costly and time consuming. Furthermore, where there is measured runoff data, typically the corresponding ASWC has not been measured. This creates a problem since ASWC is required as an input for runoff and sediment models. A possible solution is to construct a model that simulates soil water content data continuously. At present, such models include the Rangeland Hydrology and Erosion Model (RHEM) (Zhang et al., 2011a), the Bridging Event and Continuous Hydrological (BEACH) model (Vahedberdi et al., 2009), the Multiple Linear Regression (MLR) model (Liu et al., 2011), and the Water Dynamic Model (WDM) (Celestino Ladu and Zhang, 2011). Among these models, the HYDRUS-

* Corresponding author.
E-mail address: Junfan@nwsuaf.edu.cn (F. Jun).

http://dx.doi.org/10.1016/j.catena.2015.11.017
0341-8162/

1D model (Simunek et al., 2012) is based on the Richards' equation, with an added term for root water uptake. It can simulate the components of the entire soil water hydrological process including, for example, evapotranspiration, precipitation or irrigation, and deep drainage (Fan et al., 2012; Tafteh and Sepaskhah, 2012; Xu et al., 2005; Zhang et al., 2011b). This model has served an important role in studies of the vadose zone and has been used in a variety of applications (Simunek et al., 2008a).

The main objective of this study was to determine if the use of HYDRUS-1D could provide a method for predicting ASWC effects on runoff and soil erosion on the Loess Plateau where only runoff and sediment yield data existed. In order to achieve this, HYDRUS-1D was used to simulate continuous soil water contents to generate values of ASWC for rainfall-runoff events. An assessment was made of the accuracy of the model predictions of ASWC by comparing the measured and predicted data. Based on the results of this analysis, we then considered the applicability of the model for predicting ASWC on the Loess Plateau and suggested further research that could be undertaken.

2. Materials and methods

2.1. Site description

The study site was located at Shenmu Erosion and Environmental Experimental Station, Institute of Soil and Water Conservation, Ministry of Water Resources, Chinese Academy of Sciences, Northwest Agricultural and Forestry University, in Yulin City, Shaanxi Province, China (110°31′E, 38°50′N). The study site was situated in the Liudaogou watershed (110°21′–10°23′E, 38°46′–38°51′N) on the Loess Plateau. This location is in the wind–water erosion crisscross region, which is subject to severe soil erosion caused alternately by wind and water (Tang, 1990). The climate is semi-arid, which is characterized by extreme seasonal differences in temperature and precipitation. A very dry winter and spring often leads to droughts and, with typically low amounts of precipitation, the area is then susceptible to wind erosion and sandstorms. In contrast, the summers are relatively wet and are characterized by intense rain and hail storms. The concentration of the rainfall in a small number of intense rainstorms leads to floods and water erosion. The mean annual rainfall is 437.4 mm and the mean annual temperature and the mean daily maximum and minimum temperatures are 8.4 °C, 13.8 °C and 3.1 °C, respectively. The annual mean number of days with gale force winds (equal or greater to Force 8 on the Beaufort scale) is 16.2, and the annual mean number of days having dust storms is at least 4 (Li et al., 2005). The rainy season is between June and September during which approximately 80% of the total annual rainfall occurs (Zhu and Shao, 2008). The terrain is characteristically typical of the loess hilly-gully region, in which gullies formed by erosion dissect the deep loessial deposits of the Plateau.

2.2. Experiment methods

The experiment was conducted between April 2010 and September 2013. Only one set of controlled experimental conditions, with three replications, was considered in this pilot study. Three parallel experimental runoff plots (length: 12 m; width: 5 m; slope: 15°) enclosed by a cemented slab stone wall (20 cm aboveground and 30 cm underground) were established on a cultivated slope in 2002. The plots were separated by 1.5 m of bare soil. The plots were mainly planted with green beans (*Vigna radiata* (*Linn.*) *Wilczek*) during the study period according to the local farming practice. The mean crop yield over four years was 5 336 kg ha^{-1}. The leaf area index (m^2 m^{-2}) (LAI) was measured in triplicate with an LAI2000 Plant Canopy Analyzer Instrument (LI-COR Biosciences, Lincoln, U.S.A.) each week during the growing season, and belowground biomass in soil samples extracted by auguring was measured once in each plot at the end of the growing season.

A meteorological station located close to the experimental plots automatically recorded the meteorological data (rainfall amount and rainfall duration, wind speed, maximum and minimum daily temperatures, daily solar radiation) between April and October in each of the four study years. Rainfall intensity was measured using a HOBO RG3-M (Onset Computer Corporation, Bourne, U.S.A.).

The mean volumetric soil water content of the soil surface layer (0–6 cm) was measured using a Hydra Probe (Incorporated Company of Stevens Water Monitoring Systems, Portland, Oregon, U.S.A.) at 10-day intervals during the growing season in 2010 and 2012. However, in 2011 and 2013, the measurements were made, at the same intervals, only during the months of August and September. The Hydra Probe has an accuracy of ± 0.03 cm^3 cm^{-3} after it has been calibrated for the local soil. The probe conveniently measures the mean soil water content of the 0–6 cm soil layer, the thickness of which is restricted by the length of the needles of the probe, which are 6 cm long. At the time of measurement, the probe was pushed into the soil vertically and five measurements were made and averaged. Soil water contents in the soil profile (0–200 cm) was measured using a neutron probe (CNC, Beijing, China) in April, May, June, July, August, September and October in 2010 and 2012, but in April, August, and October in 2011, April, June, August, and October in 2013. These soil water content measurements were used to calibrate the HYDRUS-1D model. Antecedent soil water content was taken to be the water content simulated on the day before a rainstorm.

Runoff and sediments were funneled into collection buckets at the lower outlets of the experimental plots (Fig. 1). Pairs of collection buckets (diameter 60 cm, depth 100 cm) were positioned at two heights. When the upper bucket was full, excess runoff was split so that only one seventh of the runoff and sediment flowed into the lower bucket. This arrangement can collect samples from heavy rainstorms using small buckets. The amounts of runoff and sediments were measured after each rain event. The runoff was determined by measuring the water depth in the bucket. The contents of the bucket were then thoroughly mixed, and three 1-L subsamples were removed from each bucket during mixing. If the runoff water was less than 3 L, only the water depth was measured due to the low amount of soil erosion. The subsample was allowed to stand for 24 h to allow the sediments to settle. Excess water was decanted, and the sediment mass was then determined after oven-drying at 105 °C for 24 h.

2.3. HYDRUS-1D modeling

The HYDRUS-1D is used here to simulate soil water content, a one-dimensional variable saturation soil water model (Simunek et al., 2008b). The van Genuchten–Mualem models the variation of $K(h)$ with soil water content where

$$\theta(h) = \begin{cases} \theta_r + \dfrac{\theta_s - \theta_r}{\left[1 + |\alpha h|^n\right]^m} & h < 0 \\ \theta_s & h \geq 0 \end{cases} \tag{1}$$

$$K(h) = K_s S_e^l \left[1 - \left(1 - S_e^{1/m}\right)^m\right]^2 \tag{2}$$

where the effective saturation, S_e is

$$S_e = \frac{\theta - \theta_r}{\theta_s - \theta_r} \tag{3}$$

$$m = 1 - \frac{1}{n}, \quad n > 1 \tag{4}$$

and θ_r is the residual water content, θ_s is the saturated water content, α, n and l are empirical parameters that determine the shape of the soil water retention curve where α is related to the inverse of the air-entry suction, while n and l are related to the pore size distribution

Fig. 1. The arrangement of collection buckets at the lower outlets of the experimental plots.

and a pore-connectivity, respectively, and K_s is the saturated hydraulic conductivity.

2.3.1. Boundary conditions

The soil was a coarse-textured loessial soil. Loess is an aeolian sediment formed by the accumulation of wind-blown silt. It is usually homogeneous, highly porous and vertical capillaries are abundant, the Loess has a much higher vertical than horizontal permeability (Parsons et al., 2009; Mu et al., 2003). Based on the structure and texture of the soil, lateral movement of soil water was assumed to be negligible. The simulation run with daily time steps and the model was used to simulate the soil water movement processes in the 0–200 cm soil layers of the experimental plots because the maximum rooting depth of the green beans growing in the plots was 60 cm. The upper boundary selected was the atmospheric boundary with the surface layer, which permits water to build up on the soil surface. However, runoff did not be simulated and zero, maximum height of water at soil surface was set up in this simulation. The lower boundary was set for free drainage conditions due to the deep soil in the study where the water table is much deeper than the domain of interest. Initial condition was a measured soil water content in the soil profile using a neutron probe in April, 2010.

2.3.2. Meteorological conditions

The HYDRUS-1D model required the input of meteorological conditions such as rainfall, potential soil surface evaporation (E_p, mm d^{-1}) and potential transpiration (T_p, mm d^{-1}). Daily rainfall was input as the original rainfall minus measured runoff because runoff was not simulated. Potential soil surface evaporation (E_p) and potential transpiration (T_p) were calculated. Evapotranspiration (ET, mm d^{-1}) calculating software (Ref-ET: Reference Evapotranspiration Calculator, University of Idaho Extension, U.S.A.) based on the Penman formula used inputs of the area's meteorological data, i.e., the maximum and minimum temperatures, wind speed, and solar radiation, to calculate the reference ET (ET_0, mm d^{-1}). Typically, the E_p and T_p for the study area were calculated using the following equations (FAO, 1996):

$$T_p = ET_0\left(1 - e^{-k\cdot \mathrm{LAI}}\right) = ET_0 SCF \quad (5)$$

$$E_p = ET_0 e^{-k\cdot \mathrm{LAI}} = ET_0(1 - SCF) \quad (6)$$

where LAI is the leaf area index (dimensionless), SCF is the soil cover fraction (dimensionless), which was appropriate for the vegetation canopy of the study area; and k (dimensionless) is the radiation extinction coefficient by the canopy that was taken as 0.463 (Ritchie, 1972).

2.3.3. Plant growth condition

Factors affecting the transpiration of the plants were the aboveground and belowground biomasses. The LAI was related to the aboveground biomass and affected the ratio of leaf transpiration to evaporation (Sammis et al., 1985). The belowground biomass was directly related to the development of the plant root system, which affected water uptake by the plants. Therefore, the LAI was measured as an input to separate potential transpiration and evaporation. The root water uptake, depending on pressure head conditions at different depths actual root uptake is either equal to potential root uptake or lower was derived by using the Feddes model, using the option of "small grain" plant from the model's database, and then the determined Feddes root uptake parameters were used as the defaults. The root growth factor was calculated based on the assumption that 50% of the root depth was reached at the midpoint of the growing season. The initial root growth depth was assumed to be zero and the maximum root depth was based on measured data determined in this study from the same soil samples used to estimate below-ground biomass (Simunek et al., 2008b).

2.3.4. Calibration and validation of the model

We assumed that soil water movement would be restricted to one vertical dimension because the study site was homogeneously textured with high sand content and non-layered. 200 cm depth soil profile is described as two different layers, cultivated (0–20 cm) and undisturbed layer (20–200 cm). The initial soil hydraulic properties that were typical of the soil in the Shenmu area were considered based on the HYDURS-1D using of previous study on this soil (Fan et al., 2012). We calibrated the model using the full 4 years of data in soil profile. There were nine observed nodes from 40–200 cm soil layer, but an additional observed node was set at the depth of 3 cm which was considered as an average of 0–6 cm soil layer in the cultivated layer. The measured soil water contents in 0–30 cm did not be used to calibrate because the neutron probe soil water content measurements close to soil surface is not accurate. The inverse solution module in HYDRUS-1D optimizes the soil hydraulic parameters, α, n and K_s. The parameters used in the HYDRUS-1D model after optimization is given in Table 1.

Table 1
Characteristic parameters of soil water content.

	θ_r (cm^3 cm^{-3})	θ_s (cm^3 cm^{-3})	α (cm^{-1})	n	K_s (cm h^{-1})
0–20 cm	0.05	0.40	0.029	1.32	5.00
20–200 cm	0.05	0.40	0.020	1.30	4.16

The performance of the HYDRUS-1D model was assessed by using two criteria. First, the Nash–Sutcliffe model efficiency coefficient (NSE) (Nash and Sutcliffe, 1970) was used to assess the predictive power of the model; NSE was calculated by:

$$NSE = 1 - \frac{\sum_{i=1}^{N} (P_i - O_i)^2}{\sum_{i=1}^{N} (O_i - O_{ave})^2} \quad (7)$$

where P_i is the predicted soil water content; O_i is the observed soil water content; O_{ave} is the mean soil water content of all the observed events, and N is the number of observations, i.e., the number of measured events. Second, the root mean square error (RMSE) (Bhuyan et al., 2002), a commonly used criterion for model validation, was used to quantify the agreement between the measured data and the model predictions:

$$RMSE = \sqrt{\frac{\sum_{i=1}^{N} (O_i - P_i)^2}{N}}. \quad (8)$$

2.3.5. Statistical analysis

Simple linear regression analysis was carried out using SPSS 13.0 Version (SPSS Inc., Chicago, Illinois, U.S.A.) to study the relationships between runoff and factors that affect it, including soil water content, in particular the antecedent value. The F-test was used to test for the significance of regressions at the $P < 0.01$ level.

3. Result

3.1. Rainfall characteristics

Strong seasonal and annual variations of rainfall were observed during the study periods and most of the annual rainfall occurred in rainstorm events in the period between June and September in the years 2010 to 2013 in the Liudaogou watershed (Fig. 2). The total annual rainfall was 434 mm in 2010, 324 mm in 2011, 572 mm in 2012, and 669 mm in 2013; the maximum recorded 24 h rainfall amount of 69.7 mm occurred on 13 September 2013. Each year, 55%–70% of the annual rainfall occurred in the period of June to September, which was lower than the mean value of 80% (Zhu and Shao, 2008). We defined an erosive rainfall as one that had a total rainfall amount of at least 10 mm, because rainfall amounts of less than 10 mm produced no runoff; hence, there were 25 erosive rainfalls during the study period.

3.2. Runoff and sediment yield

Rainfall amount and the 30-min maximum intensity (I_{30}), i.e., the phase of the storm of 30-min duration during which the highest rainfall intensities occurred, had significant impacts on runoff ($P < 0.01$). There were 18 runoff events during the study period, and all the events occurred between July and September. These events resulted in a total runoff depth of 170.3 mm and a total soil loss that was equivalent to 55,572.5 kg ha^{-1} in the entire study period of 2010 to 2013. During the study period, the total rainfall was 1926.7 mm and, hence, the total runoff constituted 8.8% of the total rainfall. The experimental plots generated the most amount of runoff (50.1 mm; or 12.0% of the annual rainfall) and sediment yield (5223.7 kg ha^{-1}) in 2010 during the four study years. In 2010, there were seven rainfall events that produced runoff and sediment, which accounted for almost half of such events that occurred during the whole study period. Storm runoff exhibited statistically significant linear relationships with both rainfall amount and I_{30} (Fig. 3).

The amount of suspended sediment increased with the increases in total runoff amount (Fig. 4). There was a statistically significant linear relationship ($P < 0.01$) in the 12 m × 5 m experimental plots but, when runoff exceeded 10 mm, the suspended sediment exhibited a higher variability in the relationship with runoff. This relationship was expected since, in general, larger amounts of runoff having the same runoff rate would carry more sediment. Furthermore, where the runoff rate was increased by the more intense rainstorms, which were also associated with larger runoff amounts, the overland flow would have a greater shear force that would detach more soil particles as well as having a higher carrying capacity (An et al., 2008). However, there were two rainstorm events (on 11 August and 19 September in 2010) where relatively large amounts of runoff (27.3 mm and 16.1 mm) removed relatively little soil (3091.3 kg ha^{-1} and 1255.4 kg ha^{-1}). A possible reason for this phenomenon was the development of a soil surface seal by rainfall that occurred on two consecutive days before the runoff was actually produced. Loessial soils are susceptible to soil sealing, which results from raindrop impact and the physicochemical dispersion of soil particles (Agassi et al., 1981). A consolidated surface seal reduces the amount of small loose particles on the soil surface that are more readily removed by overland flow while forming a surface that is resistant to detachment (Bradford et al., 1987). It has also been shown by Levy et al. (1997) and Mamedov et al. (2006) that an aging effect,

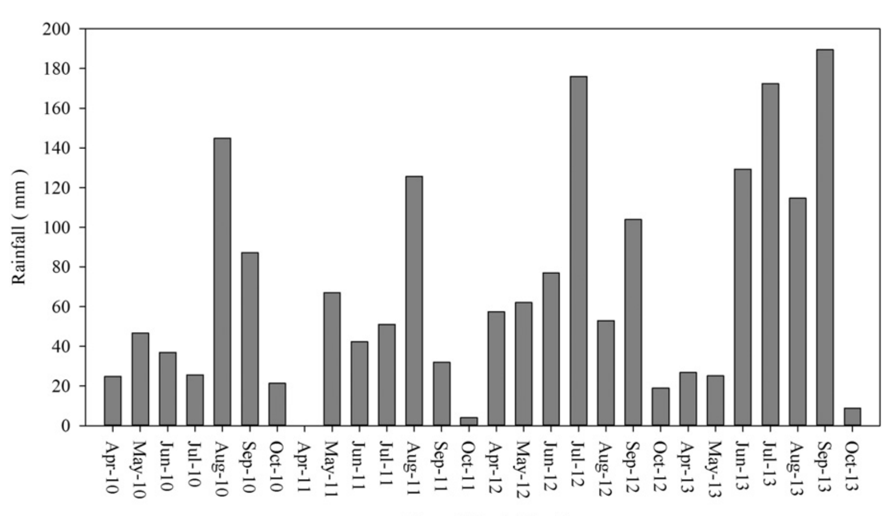

Fig. 2. Monthly rainfall during the rainy season (April to October) for 2010 to 2013.

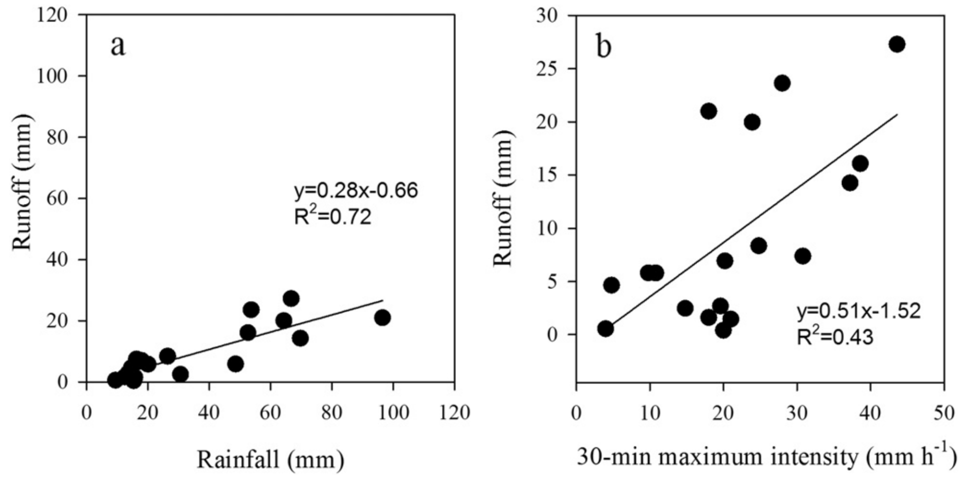

Fig. 3. Effects of (a) rainfall amount and (b) 30-min maximum intensity (i.e., the phase of the storm of 30-min duration during which the highest rainfall intensities occurred) on runoff in 2010–2013; R^2 is the determination coefficient of the linear correlations.

which in our case could be considered to occur during the low intensity rainfall period prior to the main storm that produced runoff, results in further increases in the cohesive forces between soil particles. Furthermore, other factors might have affected the amounts of runoff and sediment produced from the experimental plots. For example, vegetation likely altered soil infiltration, and dynamically affected soil surface roughness during a rainstorm. These factors are the type that often produces the most uncertain data that is the least readily available. Demonstrably, soil erosion had been significantly reduced by planting alfalfa or simply by stopping farming altogether on the same slope as the one used in this study (Fan et al., 2010). Therefore, given the complexity of the interaction of all of the above factors, temporal variation in erosion events during the study period was large.

3.3. HYDRUS-1D simulated soil water content

Fig. 5 shows that the HYDRUS-1D model simulated the daily SWC changes at 3 cm depth during the study period. The simulation exhibited the interstorm variations of SWC. The minimum and maximum SWC measured in the plots were 0.07 and 0.30 $cm^3\ cm^{-3}$, respectively. For about 6 of the 42 measurements, overestimation of SWC by the model is apparent, while underestimation occurs about four times. However, the prediction indicators and visual identification indicated that the modeled results were acceptable. Thus, the differences between the means of the measured soil water values and those produced by the model simulations were generally small. The RMSE values ranged from 0.026 to 0.037, while the NSE values for the individual study years ranged from 0.324 to 0.499, where a value of 1 would indicate the model perfectly simulated the data (Table 2). The mean NSE for the four-year study period was 0.411, which indicates that the efficiency of the model simulation was acceptable (Krause et al., 2005).

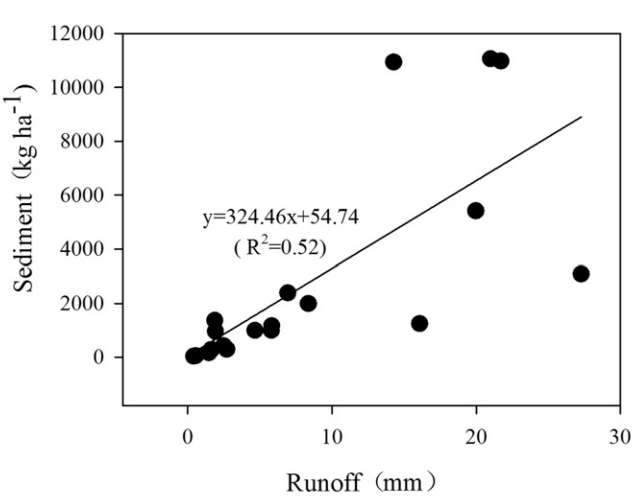

Fig. 4. Relationship between runoff and sediment yield during 2010–2013; R^2 is the determination coefficient of the linear correlation.

3.4. Relationships between antecedent soil water content and runoff

The probability of generating runoff was affected by different ASWCs. If ASWC was greater than 0.12 $cm^3\ cm^{-3}$, 85% of the erosive rainfalls produced runoff. Runoff tended to increase with the increase in the antecedent soil water content (ASWC) that was determined by the HYDRUS-1D model, but the relationship was not statistically significant ($P = 0.14$; Fig. 6a). However, there were three rainfall events that generated very high runoff amounts when the ASWCs were relatively low. The measured meteorological data showed that the 30-min maximum intensities of these three events were greater than 24 mm h^{-1} and that the amounts of rainfall were greater than 54 mm. The crop was growing well when these events occurred on 11 August 2010, 19 August 2011, and 21 July 2012. When the rainfall amount and intensity are both relatively high, the steady state phase of the infiltration process would affect total runoff to a greater extent than the effect of ASWC, which would become less significant (Castillo et al., 2003). Since such highly erosive rainfall events are rare in the study region, accounting for only 12% of all rainstorms, it was decided to examine the relationship between runoff and ASWC after these three aberrant events were removed from the dataset. Under these field conditions, aberrant events were considered to have occurred when the rainfall amount exceeded 54 mm and the runoff amount was greater than 20 mm. After doing so, ASWC was found to be significantly correlated to the runoff amount (determination coefficient, $R^2 = 0.62$; $P < 0.01$) (Fig. 6b). This indicates that runoff was directly affected by ASWC in most of the rainfall-runoff events occurring during this study.

4. Discussion

4.1. The capability of the HYDRUS-1D model to simulate the soil water content

The model performed well, although the NSE value differed among the study years. The NSE was lower in 2011 and 2012 than in 2010 and 2013. However, the simulated soil water content was comparable

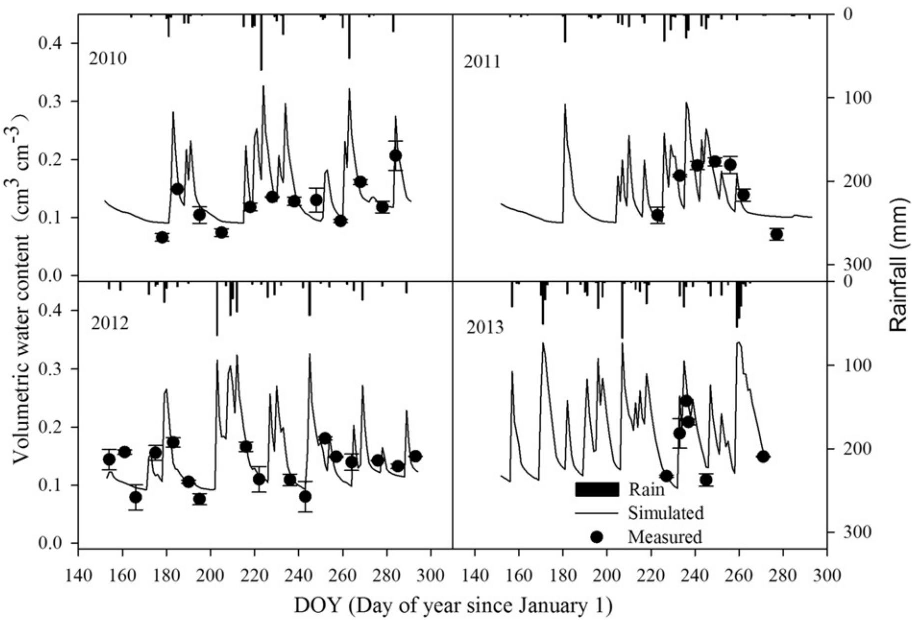

Fig. 5. Simulated and measured water contents in the 0–6 cm soil layer for the four study years (2010–2013).

Table 2
Prediction indicators of the HYDRUS-1D model simulation of soil water content in the 0–6 cm soil layer between 2010 and 2013.

	2010	2011	2012	2013	Mean
NSE[a]	0.486	0.324	0.334	0.499	0.411
RMSE	0.026	0.037	0.026	0.034	0.031
n	12	7	17	6	

RMSE, root mean square error; n, sample number.
[a] NSE, Nash–Sutcliffe efficiency.

to measured results over all four years. Soil type and LAI were the key parameters affecting model performance (Chen et al., 2014). Therefore, soil parameters could be used for a particular soil texture over a long period after corrections and validations had been made using an observational database. Meteorological data, which includes air temperature, solar radiation, humidity, wind speed and rainfall, is relatively easy to collect from local meteorological stations. The data requiring in situ measurements are the LAI, root depth and SWC. However, for a given site and crop species, the long-term mean seasonal changes of LAI and root depth can be substituted for in situ measurements of these plant parameters in the HYDRUS-1D simulations. Simple vegetation characterizations, such as the use of those two parameters, does appear to cause problems with estimations of water lost in plant transpiration, especially from the deeper soil layers. However, SWC has been better simulated by HYDRUS-1D for upper soil layers than for full soil profiles (Chen et al., 2014). Therefore, the performance of the HYDRUS-1D in modeling the changes in the SWC of the upper 0–6 cm soil layer in this study area was reasonable, and values of ASWC could be obtained that were considered to be reliable. It is better to monitor soil water content in situ automatically, which would improve the calibration and validation of the model. In addition, many studies have shown that the HYDRUS-1D model can simulate soil water content well in many diverse locations around the world over a wide range of conditions, such as soil type and climate and degree of vegetation cover (Fan et al., 2012; Simunek et al., 2008c; Xu et al., 2005; Zhang et al., 2011b).

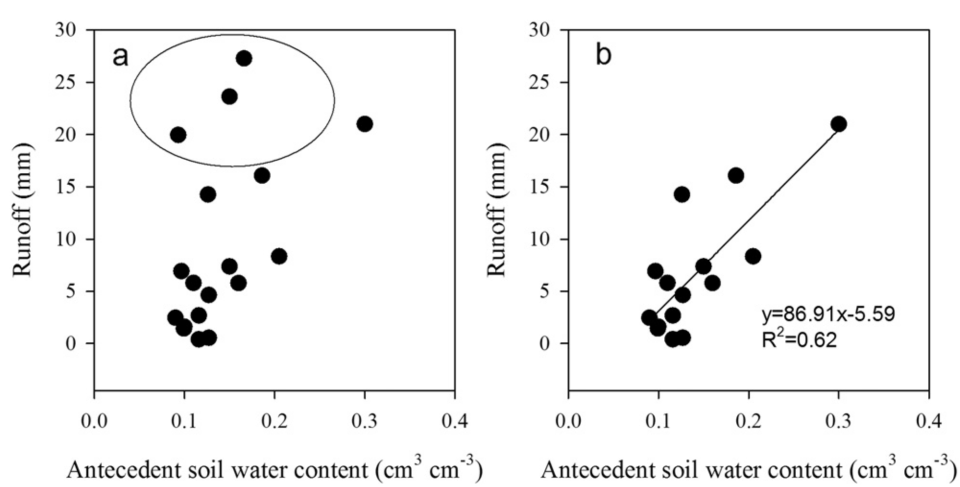

Fig. 6. Relationships between the antecedent soil water content (taken as the measured soil water content on the day before a rainstorm event) and runoff with (a) all the data included and (b) the three aberrant rainfall-runoff events (in the circle) removed; R^2 is the determination coefficient of the linear correlation.

4.2. ASWC influences on runoff and sediment yield

Many studies have shown that the factors affecting runoff and sediment yield include slope gradient, rainfall intensity and vegetation coverage (Huang et al., 2010; Huang et al., 2013; Nadal-Romero et al., 2015; Peng and Wang, 2012; Wei et al., 2007b). Even though increases in slope gradient and rainfall intensity increased the sediment yield and sediment concentration, the actual contributions were also dependent on soil type and the ASWC (Defersha and Melessa, 2012). Vahabi and Nikkami (2008) found that sediment yield was linearly and positively correlated to slope gradient, vegetation coverage, ASWC, and sand content under the conditions of a given rainfall intensity. Higher ASWCs also resulted in more intense erosion in this study. In a semiarid region such as the Loess Plateau, the predominant runoff mechanism is the overland flow resulting when rainfall intensity exceeds the soil infiltration capacity. For such a mechanism, the ratio of rainfall intensity to the soil hydraulic conductivity determines the generation of overland flow. The increase of soil infiltration capacity due to lower levels of SWC would reduce soil erosion in the water–wind crisscross region of the Loess Plateau. Runoff may be caused by continuous rainfall for several days because a greater volume of precipitation falls later in the storm meaning that most of rain falls on wet soil, which is more saturated. For example, there were 4 rainfall events from 3 August to 11 August in 2010 that led to three runoff events. Furthermore, the consecutive rainstorms also produced the highest amount of runoff (27.3 mm on 11 August 2010) during the four years. Another high runoff event (16.0 mm) occurred on 19 September 2010. This runoff event was also affected by the preceding rainfall event of 17 September 2010. The highest amount of runoff in this year was affected by these two large events, indicating that runoff was also controlled by the non-uniform distribution of rainfall in this region. However, for high intensity events, especially for those with high rainfall amounts (the rainfall events of 35 and 25 mm), the rainfall intensity (50 mm h^{-1}) far exceeded the soil infiltration capacity regardless of the ASWC (Castillo et al., 2003). In this study, three out of the 18 rainfall-runoff events did not relate to ASWC because of their high rainfall intensities (30-min maximum $>$24 mm h^{-1}) and high total rainfall amounts ($>$54 mm).

Previous studies have clarified the relationship between ASWC and soil erosion in small watersheds (Bowyer-Bower, 1993; Brocca et al., 2008; Castillo et al., 2003; Radatz et al., 2013; Truman et al., 2011; Zhang et al., 2011b). The addition of soil water content data for the upper 10-cm soil layer to a database that also includes rainfall could improve the runoff predictive capability of the generalized regression neural network model for 13-km^2 and 137-km^2 catchments (Tayfur et al., 2014). At the small watershed scale, the averaged ASWC of the upper 5-cm soil layer has often been used for runoff modeling. This is because it has been difficult to ascertain the actual SWC at different locations within the watershed (Zhang et al., 2011a) where SWC would probably be distinctly different due to a variety of land use patterns (Fan et al., 2010; Shi et al., 2013; Wang et al., 2013). The impact of ASWC on soil erosion was verified at the small plot scale in this study after ASWC was simulated by the model. The generation of runoff under less intense storms is not fully dependent on the ratio of rainfall intensity to infiltration but the saturation of the top soil is important (Castillo et al., 2003; Martinez-Mena et al., 1998). The close relationship between ASWC and runoff indicated that saturation-excess overland flow, more dependent on ASWC than the infiltration-excess, happened more frequently in soils with higher permeability. Similar results at the hillslope scale were reported by Scherrer et al. (2007) and Ruggenthaler et al. (2015).

It would be relatively simple to run individual HYDRUS-1D simulations for each typical land use within a catchment. This would then facilitate the investigation of the relationship between ASWC and soil erosion as well as to its spatial variability within a watershed. Therefore, the use of the HYDRUS-1D model as a tool in runoff and erosion studies can help to investigate the effect of changes in infiltration caused by various factors on overland flow. For example, in coarse textured soils on the Loess Plateau, soil water can be depleted after changing the land use from cropland to shrubland or forest plantations. The storage deficit can become high enough that more rainfall goes into soil storage and less is lost as runoff (Farrick and Branfireun, 2014). This might suggest that the cause of the reduced runoff observed following such a land use change is due to the dryer soil profile resulting from the higher was consumption of the more recent vegetation rather than or in addition to the effect of the plants on the water flow on the slopes. This hypothesis may be validated in future studies on the Chinese Loess Plateau. Large-scale ecological restoration programs on the Plateau have introduced vegetation that has drastically decreased deep soil water storage relative to that in farmland and native grassland Wang et al., 2013; Yang et al., 2014). At the regional scale, deep soil desiccation has been observed under forests, shrubland and pastures (Chen et al., 2008; Wang et al., 2011). However, because water movement into and within the soil matrix is also important for runoff generation from highly permeable soils that remain unsaturated, this desiccation can result in more rainwater entering and being redistributed within the soil profile and this water can then be used by the plants (Farrick and Branfireun, 2014). Furthermore, the HYDRUS-1D model is capable of simulating the soil water content in different soil layers. This is useful for determining the thickness of the upper soil layers where the water content has an effect on the relationship between ASWC and runoff. These issues should be investigated in the future.

5. Conclusion

Soil water content is one of many factors controlling runoff on the Loess Plateau. The ASWC can be an important factor in determining the runoff amount and sediment yields. This study was carried out to determine if the HYDRUS-1D model could accurately predict the soil water content and reasonable values of ASWC. Based on measured data collected at intervals during a four-year period, the HYDRUS-1D model was found to simulate soil water content reasonably well (mean NSE $= 0.411$) in the upper soil layer (0–6 cm) of farmland on a watershed slope. The model provided continuous parameter values, including ASWC, which could be used to predict runoff and sediment yield from hillslopes. Runoff and sediment yield increased with the increase of rainfall amount and with ASWC. When the ASWC was greater than 0.12 $cm^3\ cm^{-3}$, the probability of generating runoff could be as great as 85% when the rainfall amounts exceeded 10 mm in the study area during the study period. Therefore, the HYDRUS-1D model was considered to be a viable means by which to determine ASWC and other parameters that could then be used in models to predict erosion and runoff on the Loess Plateau.

Acknowledgments

We acknowledge funding by the National Natural Science Foundation of China (Nos. 51239009, 41271239). We are grateful to two anonymous reviewers for their helpful suggestions as well as to the editorial staff of CATENA.

References

Agassi, M., Shainberg, I., Morin, J., 1981. Effect of electrolyte concentration and soil sodicity on infiltration-rate and crust formation. Soil Sci. Soc. Am. J. 5, 848–851.
An, S.S., Zheng, F.L., Zhang, F., Pelt, S.V., Hamer, U., Makeschin, F., 2008. Soil quality degradation processes along a deforestation chronosequence in the Ziwuling area, China. Catena 75, 248–256.
Bhuyan, S.J., Kalita, P.K., Janssen, K.A., Barnesa, P.L., 2002. Soil loss predictions with three erosion simulation models. Environ. Model Softw. 17 (2), 137–146.
Bowyer-Bower, T.A.S., 1993. Effects of rainfall intensity and antecedent moisture on the steady-state infiltration rate in a semi-arid region. Soil Use Manag. 9 (2), 69–76.
Bradford, J.M., Ferris, J.E., Remley, P.A., 1987. Interrill soil erosion processes: I. Effect of surface sealing on infiltration, runoff, and soil splash detachment. Soil Sci. Soc. Am. J. 51 (6), 1566–1571.
Brocca, L., Melon, F., Moramarco, T., 2008. On the estimation of antecedent wetness conditions in rainfall-runoff modeling. Hydrol. Process. 22, 629–642.

Brocca, L., Melon, F., Moramarco, T., Morbidelli, R., 2009. Soil moisture temporal stability over experimental areas in central Italy. Geoderma 148, 364–374.

Calamita, G., Brocca, L., Perrone, A., Piscitelli, S., Lapenna, V., Melone, F., Moramarco, T., 2012. Electrical resistivity and TDR methods for soil moisture estimation in central Italy test-sites. J. Hydrol. 454, 101–112.

Castillo, V.M., Gomez-Plaza, A., Martinez-Mena, M., 2003. The role of antecedent soil water content in the runoff response of semiarid catchments: a simulation approach. J. Hydrol. 284, 114–130.

Celestino Ladu, J.L., Zhang, D.R., 2011. Modeling atrazine transport in soil columns with HYDRUS-1D. Water Sci. Eng. 4 (3), 258–269.

Chen, H.S., Shao, M.A., Li, Y.Y., 2008. Soil desiccation in the Loess Plateau of China. Geoderma 143, 91–100.

Chen, M., Willgoose, G.R., Saco, P.M., 2014. Spatial prediction of temporal soil moisture dynamics using HYDRUS-1D. Hydrol. Process. 28, 171–185.

Defersha, M.B., Melessa, A.M., 2012. Effect of rainfall intensity, slope and antecedent moisture content on sediment concentration and sediment enrichment ratio. Catena 90, 47–52.

Duiker, S.W., Flangman, D.C., Lal, R., 2000. Erodibility and infiltration characteristics of five major soils of south-west Spain. Catena 45 (2), 103–121.

Fan, J., Jones, S.B., Qi, L.B., Wang, Q.J., Huang, M.B., 2012. Effects of precipitation pulses on water and carbon dioxide fluxes in two semiarid ecosystems: measurement and modeling. Environ. Earth Sci. 67, 2315–2324.

Fan, J., Shao, M.A., Wang, Q.J., Jones, S.B., Reichardt, K., Cheng, X.R., Fu, X.L., 2010. Toward sustainable soil and water resources use in China's highly erodible semi-arid Loess Plateau. Geoderma 155, 93–100.

FAO, 1996. Drainage of irrigated lands. Irrig. Water Manag. Training Manual 9.

Farrick, K.K., Branfireun, B.A., 2014. Soil water storage, rainfall and runoff relationships in a tropical dry forest catchment. Water Resour. Res. 50, 9236–9250. http://dx.doi.org/10.1002/2014WR016045.

Fu, B.J., Liu, Y., Lu, Y.H., He, C.S., Zeng, Y., Wu, B.F., 2011. Assessing the soil erosion control service of ecosystems change in the Loess Plateau of China. Ecol. Complex. 8, 284–293.

Fu, B.J., Wang, Y.F., Lu, Y.H., Chen, L.P., Song, C.J., 2009. The effects of land use combinations on soil erosion: a case study in the Loess Plateau of China. Prog. Phys. Geogr. 33 (6), 793–804.

Gao, X.D., Wu, P.T., Zhao, X.N., Shi, Y.G., Wang, J.W., Zhang, B.Q., 2011. Soil moisture variability along transects over a well-developed gully in the Loess Plateau, China. Catena 87, 357–367.

Higgitt, D.L., 1991. Soil erosion and soil problems. Prog. Phys. Geogr. 15, 91–100.

Huang, M.B., Gallichand, J., Dong, C.Y., Wang, Z.L., Shao, M.A., 2007. Use of soil moisture data and curve number method for estimating runoff in the Loess Plateau of China. Hydrol. Process. 21, 1471–1481.

Huang, Z.G., Ouyang, Z.Y., Li, F.R., Wang, X., 2010. Response of runoff and soil loss to reforestation and rainfall type in red soil region of southern China. J. Environ. Sci. 22 (11), 1765–1773.

Huang, J., Wu, P.T., Zhao, X.N., 2013. Effects of rainfall intensity, underlying surface and slope gradient on soil infiltration under simulated rainfall experiments. Catena 104, 93–102.

Huet, J., Druilhe, C., Trémier, A., 2012. The impact of compaction, moisture content, particle size and type of bulking agent on initial physical properties of sludge-bulking agent mixtures before composting. Bio Resour. Technol. 114, 428–436.

Huo, Z., Shao, M.A., Horton, R., 2008. Impact of gully on soil moisture of shrubland in wind–water erosion crisscross region of the Loess Plateau. Pedosphere 18 (5), 674–680.

Krause, P., Boyle, D.P., Base, F., 2005. Comparison of different efficiency criteria for hydrological model assessment. Adv. Geosci. 5, 89–97.

Lal, M., Mishra, S.K., Pandey, A., 2015. Physical verification of the effect of land feature and antecedent moisture on runoff curve number. Catena 133, 318–327.

Levy, G.J., Levin, J., Shainberg, I., 1997. Prewetting rate and aging effects on seal formation and interrill soil erosion. Soil Sci. 162 (2), 131–139.

Li, M., Li, Z.B., Liu, P.L., Yao, W.Y., 2005. Using Cesium-137 technique to study the characteristics of different aspect of soil erosion in the wind–water erosion crisscross region on Loess Plateau of China. Appl. Radiat. Isot. 62, 109–113.

Liu, H., Lei, T.W., Zhao, J., Yuan, C.P., Fan, Y.T., Qu, L.Q., 2011. Effects of rainfall intensity and antecedent soil moisture on soil infiltrability under rainfall conditions using the run off-on-out method. J. Hydrol. 396, 24–32.

Mamedov, A.I., Huang, C., Levy, G.J., 2006. Antecedent moisture content and aging duration effects on seal formation and erosion in Smectitic soil. Soil Sci. Soc. Am. J. 70, 832–843.

Martinez-Mena, M., Albaladejo, J., Castillo, V., 1998. Factors influencing surface runoff generation in a Mediterranean semiarid environment: Chicamo watershed, SE Spain. Hydrol. Process. 12, 741–754.

Mu, X., Xu, X., Wang, W., Wen, Z., Du, F., 2003. Impact of artificial forest on soil moisture of the deep soil layer on Loess Plateau. Acta Pedol. Sin. 40, 210–217.

Nadal-Romero, E., González-Hidalgoa, J.C., Cortesia, N., Desirc, G., Gómez, J.A., Lasanta, T., Lucíaf, A., Marín, C., Martínez-Murillo, J.F., Pachecoh, E., Rodríguez-Blancoi, M.L., Díazj, A.R., Ruiz-Sinoga, J.D., Taguas, E.V., Taboada-Castro, M.M., Taboada-Castroi, X., Úbeda, X., Zabaleta, A., 2015. Relationship of runoff, erosion and sediment yield to weather types in the Iberian Peninsula. Geomorphology 228, 372–381.

Nash, J., Sutcliffe, J., 1970. River flow forecasting through conceptual models; part I-A discussion of principles. J. Hydrol. 10 (3), 282–290.

Ni, S.X., Ma, G.B., Wei, Y.C., Jiang, H.F., 2004. An indicator system for assessing soil erosion in the Loess Plateau gully regions: a case study in the Wangdonggou Watershed, China. Pedosphere 14 (1), 37–44.

Paola, F.D., Ranucci, A., Feo, A., 2013. Antecedent moisture condition (SCS) frequency assessment: a case study in Southern Italy. Irrig. Drain. 62 (Supplement 2), 61–71.

Parsons, R.L., Johnson, R.M., Brown, D.A., Dapp, S., Brennan, J.J., 2009. Characterization of Loess for deep foundations. DFI J. 3 (2), 11–21.

Peng, T., Wang, S.J., 2012. Effects of land use, land cover and rainfall regimes on the surface runoff and soil loss on karst slopes in southwest China. Catena 90, 53–62.

Qiu, Y., Fu, B.J., Wang, J., Chen, L.D., 2001. Spatial variability of antecedent soil moisture and its relation to environmental indices in a semi-arid gully catchment of the Loess Plateau, China. J. Arid Environ. 49, 723–750.

Qiu, Y., Fu, B.J., Wang, J., Chen, L.D., 2003. Spatiotemporal prediction of soil moisture content using multiple-linear regression in a small catchment of the Loess Plateau, China. Catena 54, 173–195.

Radatz, T.F., Thompson, A.M., Madison, F.W., 2013. Soil moisture and rainfall intensity thresholds for runoff generation in southwestern Wisconsin agricultural watersheds. Hydrol. Process. 27, 3521–3534.

Ritchie, J.T., 1972. Model for predicting evaporation from a row crop with incomplete cover. Water Resour. Res. 8 (5), 1204–1213.

Ruggenthaler, R., Schoberl, F., Markart, G., Klebinder, K., Hammerle, A., Leitinge, G., 2015. Quantification of soil moisture effects on runoff formation at the hillslope scale. J. Irrig. Drain. Eng., 05015001 http://dx.doi.org/10.1061/(ASCE)IR.1943–4774.0000880.

Sammis, T.W., Williams, S., Smeal, D., Kallsen, C.E., 1985. Effect of soil moisture stress on leaf area index, evapotranspiration and modeled soil evaporation and transpiration. Am. Soc. Agric. Eng. 29 (4), 956–961.

Scherrer, S., Naef, F., Faeh, A.O., Cordery, I., 2007. Formation of runoff at the hillslope scale during intense precipitation. Hydrol. Earth Syst. Sci. 11, 907–922.

Shi, Z.H., Ai, L., Li, X., Huang, X.D., Wu, G.L., Liao, W., 2013. Partial least-squares regression for linking land-cover patterns to soil erosion and sediment yield in watersheds. J. Hydrol. 498, 165–176.

Simunek, J., Köhne, J.M., Kodešová, R., Šejna, M., 2008c. Simulating nonequilibrium movement of water, solutes, and particles using HYDRUS: a review of recent applications. Soil Water Res. 3 (1), S42–S51.

Simunek, J., Sejna, M., Saito, H., Sakai, M., van Genuchten, M.T., 2008b. The HYDRUS-1D Software Package for Simulating the One-dimensional Movement of Water, Heat, and Multiple Solutes in Variably-saturated Media. Version 4.0, HYDRUS Software Series 1. Department of Environmental Science, University of California Riverside, Riverside, California, p. 281.

Simunek, J., Genuchten, M.T.V., Šejna, M., 2008a. Development and applications of the HYDRUS and STANMOD software packages and related codes. Vadose Zone J. 7, 587–600.

Simunek, J., Genuchten, M.T.V., Šejna, M., 2012. HYDRUS: model use, calibration, and validation. Am. Soc. Agric. and Biol. Eng. 55 (4), 1261–1274.

Tafteh, A., Sepaskhah, A.R., 2012. Application of HYDRUS-1D model for simulating water and nitrate leaching from continuous and alternate furrow irrigated rapeseed and maize fields. Agric. Water Manag. 113, 19–29.

Tang, K.L., 1990. Soil Erosion on the Loess Plateau and Its Control. China Science and Technology Press, Beijing (in Chinese).

Tayfur, G., Zucco, G., Brocca, L., Moramarco, T., 2014. Coupling soil moisture and precipitation observations for predicting hourly runoff at small catchment scale. J. Hydrol. 510, 363–371.

Truman, C.C., Potter, T.L., Nuti, R.C., Franklin, D.H., Bosch, D.D., 2011. Antecedent water content effects on runoff and sediment yields from two Coastal Plain Ultisols. Agric. Water Manag. 98, 1189–1196.

Vahabi, J., Nikkami, D., 2008. Assessing dominant factors affecting soil erosion using a portable rainfall simulator. Int. J. Sediment Res. 23, 376–386.

Vahedberdi, S., Saskia, V., Leo, S., 2009. A simple model to predict soil moisture: Bridging Event and Continuous Hydrological (BEACH) modeling. Environ. Model Softw. 24, 542–556.

Wang, S., Fu, B.J., Gao, G.Y., Liu, Y., Zhou, J., 2013. Responses of soil moisture in different land cover types to rainfall events in a re-vegetation catchment area of the Loess Plateau, China. Catena 101, 122–128.

Wang, Y.Q., Shao, M.A., Zhu, Y.J., Liu, Z.P., 2011. Impacts of land use and plant characteristics on dried soil layers in different climatic regions on the Loess Plateau of China. Agric. For. Meteorol. 151 (4), 437–448.

Wei, W., Chen, L.D., Fu, B.J., Huang, Z.L., Wu, D.P., Gui, L.D., 2007b. The effect of land uses and rainfall regimes on runoff and soil erosion in the semi-arid loess hilly area, China. J. Hydrol. 335, 247–258.

Wei, L.H., Zhang, B., Wang, M.Z., 2007a. Effects of antecedent soil moisture on runoff and soil erosion in alley cropping systems. Agric. Water Manag. 94, 54–62.

Xu, L.G., Yang, J.S., Zhang, Q., Liu, G.M., 2005. Salt-water transport in unsaturated soils under crop planting: dynamics and numerical simulation. Pedosphere 15 (5), 634–640.

Yang, L., Chen, L.D., Wei, W., Yu, Y., Zhang, H.D., 2014. Comparison of deep soil moisture in two re-vegetation watersheds in semi-arid regions. J. Hydrol. 513, 314–321.

Zhang, J., Gong, H.L., Mark, A.R., Li, X.J., Zhou, D.M., 2011b. Numerical modeling of shallow water table behavior with Lisse effect. Chin. Geogr. Sci. 21 (2), 249–256.

Zhang, Y., Wei, H., Nearing, M.A., 2011a. Effects of antecedent soil moisture on runoff modeling in small semiarid watersheds of southeastern Arizona. Hydrol. Earth Syst. Sci. 15, 13172–13179.

Zheng, F.L., 2006. Effects of vegetation changes on soil erosion on the Loess Plateau. Pedosphere 16, 420–427.

Zhu, Y.J., Shao, M.A., 2008. Spatial distribution of surface rock fragment on hillslopes in a small catchment in wind–water erosion crisscross region of the Loess Plateau. Sci. China Ser. D Earth Sci. 51 (6), 862–870.